Is Au_{55} or Au_{38} Cluster a Threshold Catalyst for Styrene Epoxidation?

W. Gao, X. F. Chen, J. C. Li, and Q. Jiang*

Key Laboratory of Automobile Materials, Ministry of Education, and School of Materials Science and Engineering, Jilin University, Changchun 130022, China

Received: September 29, 2009; Revised Manuscript Received: November 1, 2009

The styrene epoxidation on Au_{38} and Au_{55} clusters, which could be a benchmark to probe high catalytic activity of gold clusters, has been studied by using density functional theory. Results suggest that epoxidation proceeds via a surface oxametallacycle intermediate (OME structure). Two parallel reaction pathways coexist on the Au_{38} cluster: O_2 dissociates before epoxidation and O_2 directly reacts with styrene, whereas only the latter pathway is found on the Au_{55} cluster, which is induced by different geometries of the Au_{38} and Au_{55} clusters. The mechanism of O_2 directly reacting is essentially determined by the electronic resonance between electronic states of adsorbed intermediates and Au atoms at reaction sites. Moreover, Au atoms correlated with the reaction on the Au_{38} cluster are more electropositive than those on the Au_{55} cluster, which leads to a higher catalytic activity of the former. Thus, the Au_{38} cluster should be the size threshold for epoxidation catalysis, being consistent with the obtained barrier values.

1. Introduction

Bulk gold is an inert metal and has long been viewed as catalytically inactive. Since the pioneering work of Haruta and co-workers,[1,2] Au clusters have been demonstrated to be a good catalyst for many important reactions, especially the epoxidation of propene[3] and selective oxidations of methanol and styrene.[4–7] It is noteworthy that, although smaller Au clusters are generally more active for catalysis, supported Au particles with a diameter of 10−20 nm as an exception are found to be more active than the smaller ones for selective hydrogenation of but-2-enal.[8] This is partly induced by the appearance of the ZnO support where supported gold nanoparticles have shown unusual and somewhat unexpected catalytic properties.[9–13] It is suggested that the quantum size effects and factors,[10,14–18] such as thickness, shape, and oxidation state,[19–23] of gold particles are responsible for their high catalytic activity. In addition, the strong electronic interaction between Au and the dioxide support also affects the reactivity of supported Au. The origin of the catalytic activity, however, is still not fully understood.

A striking size threshold effect associated with a metal-to-insulator transition of Au particles supported on $TiO_2(110)$ has been experimentally found, which shows that Au particles are catalytically active only when their diameter (D) is below 3.5 nm.[10] Experimental works also indicates that Au clusters with 55 atoms (Au_{55}) supported on inert substrates are efficient and robust catalysts for the selective oxidation of styrene by dioxygen.[7] It is suggested that these Au entities can dissociatively chemisorb O_2 to yield O adatoms that are necessary for triggering subsequent catalytic chemistry. Moreover, there is a sharp size threshold of about $D = 2$ nm of those particles in catalytic activity, whereas that above is completely inactive.[7] Also, the catalytic activity arises from altered electronic structures intrinsic to Au clusters. This inspires us to explore the origin of size threshold of Au clusters in catalytic activity. Moreover, although the epoxide products are versatile intermediates in the chemical industry, the mechanism of epoxidation is also controversial. Styrene can be easily epoxidized by O atoms, and the surface oxametallacycle intermediate (OMME) plays a key role in the reaction,[24,25] where OMME is a ring structure including a −C−C−O− framework and two Au atoms. Moreover, it is proposed that chlorine can significantly enhance the selectivity of styrene epoxidation by changing the geometric arrangement of the O-covered Au surface.[26] The epoxidation mechanism is, however, unclear yet, such as the active oxygen species, and the effect of Au topography.

In this paper, the styrene epoxidation on Au clusters is simulated using DFT technique. The dissociation of chemisorbed O_2 to O adatom is first considered. Afterward, the selective oxidation of styrene is calculated. The minimum energy pathway is determined by comparing their corresponding barrier energies (E_a). Moreover, the atomic and electronic structures of the transition state (TS) and intermediates are also calculated to explain the size threshold in catalytic activity for Au clusters.

2. Calculations

DFT simulations have been performed using DMOL^3 code.[27,28] The generalized gradient approximation (GGA) with the Perdew−Burke−Ernzerhof (PBE) functional is employed as the exchange-correlation functional.[29] The core treatment method of DFT semicore pseudopots (DSPP) is included in all calculations (the pseudopotential including a local part and a nonlocal one),[28] where the effect of core electrons is substituted by a simple potential, including some degree of relativistic effects.[30] This technique is computationally inexpensive and is a very useful approximation for elements with an atomic number being more than 21. In the DMOL method, the physical wave functions are expanded in terms of accurate numerical basis sets.[27,28] A double numerical plus polarization (DNP) is employed where double numerical (DN) is used in DNP by analogy with Gaussian double-ζ sets. In DNP, besides DN, there is additionally a polarization p-function on all hydrogen atoms. The size of the DNP basis set is comparable to Gaussian 6-31G**, but DNP is more accurate than a Gaussian basis set of the same size.[31,32] These settings yield a convergence tolerance of energy of 2.0×10^{-5} hartree (Ha) (1 Ha = 27.2114

* To whom correspondence should be addressed. Fax: 86-431-85095876. E-mail: jiangq@jlu.edu.cn.

10.1021/jp909345j
Published on Web 11/24/2009

TABLE 1: Adsorption Energy (E_{ad}) of O_2 on Au_{55} and Au_{38} Clusters at Different Sites[a]

		T_1	T_2	B_1	B_2	H_1	H_2
55	E_{ad}	0.23	0.07	0.34	0.34	0.26	0.11
	E_a	2.88	3.02	1.55	1.57	1.33	1.41
		T_1	B_1	B_2	B_3	H_1	H_2
38	E_{ad}	0.36	0.57	0.47	0.29	0.41	0.32
	E_a	2.45	1.73	1.29	0.73	1.31	1.46

[a] For the meanings of T, B, and H, see the caption of Figure 1.

eV), a maximum force of 0.004 Ha/Å, and a maximum displacement of 0.005 Å.

To detect the structure of the Au_{55} cluster on an inert substrate, a BN(111) $P(6 \times 5)$ structure is utilized, which includes three layers with two bottom layers fixed. The vacuum distance is more than 16 Å. In the initial state, one of the triangle surfaces in the Au_{55} cluster is parallel to the BN(111) surface. The *k*-point is $1 \times 1 \times 1$ for all calculations. Note that the cluster in this work is in a free structure, unless we proclaim.

To investigate the minimum energy pathway for the O_2 dissociation, linear synchronous transit/quadratic synchronous transit (LST/QST) and nudged elastic band (NEB)[33] tools in DMOL[3] code are utilized, which have been well-validated to find a TS structure and the minimum energy pathway.

The adsorption energy E_{ad} is computed by

$$E_{ad} = -(E_{x/s} - E_x - E_s) \quad (1)$$

where the subscript *x* denotes a molecule with a certain structure, *s* shows Au(111) surface structure, while *x*/*s* shows the corresponding adsorbed system.

3. Results and Discussion

The correlated data for the adsorption and dissociation of chemisorbed O_2 on the Au_{55} cluster are calculated and shown in Table 1. There are together six possible adsorption sites on the cluster shown in Figure 1.1.1, where the Au_{55} cluster suffers hardly any distortion after O_2 adsorption. The most stable adsorption site for O_2 is B_1 through both oxygen atoms binding to Au atoms with $E_{ad} = 0.34$ eV, which is identical with reference data of $E_{ad} = 0.33$ eV.[34] The E_{ad} was also suggested to be about 0.06 eV (6 KJ/mol) on the Au_{55} cluster,[35] which should correspond to that adsorbed on a step site (T_2) in our calculation. For O_2 dissociation, Figure 1.1.3 shows the common TS structure for O_2 dissociation at all sites. Importantly, no surface Au atoms are shared between the two O atoms, which is in agreement with the cases on Au steps, kinks, and a Au_{29} cluster.[18] This structure can avoid large repulsive interaction between two O atoms at the TS due to the bonding competition effect, thus decreasing the barrier. However, $E_a > 1.33$ eV on these sites.

We further study the case of O_2 on the Au_{38} cluster, being similar to that on the Au_{55} cluster. O_2 is weakly adsorbed on Au_{38} ($E_{ad} < 0.57$ eV) with a high dissociation barrier ($E_a > 0.73$ eV). The previous results also suggested that $E_a > 1$ eV for Au clusters with a size ranging from 12-atom ($D < 1$ nm) to 48-atom ($D \sim 1-2$ nm),[18] although O_2 can dissociate easily by the presence of some atomic oxygen or on an unsupported Au_{10} cluster.[36,37] The latter is due to the release of Au atoms from the surface restructuring induced by atomic oxygen deposition or a particular size and shape. This means that O_2 is desorbed on these clusters before dissociation. Namely, O_2 is hardly dissociated on Au_{55} and Au_{38} clusters. Note that the possibility

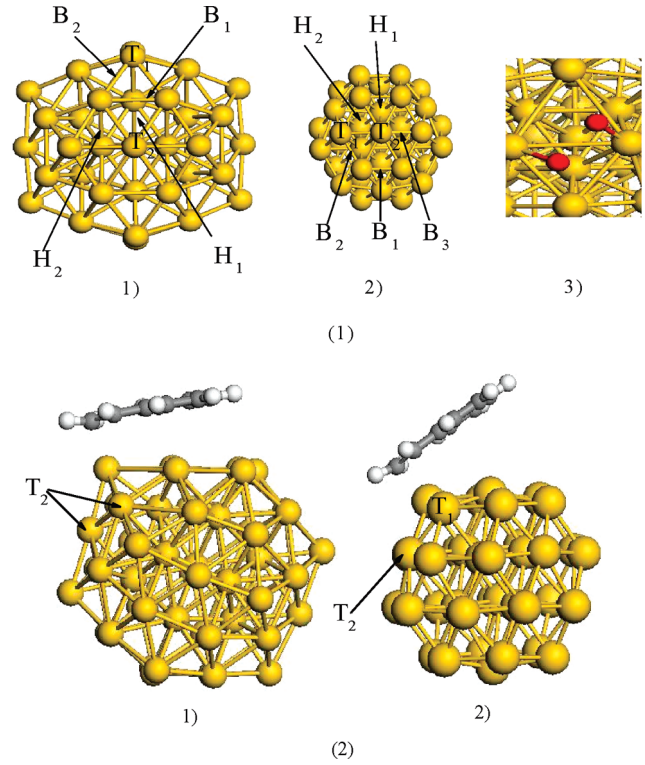

Figure 1. Parameter of adsorption sites, TS structure, and styrene adsorbed structures on Au_{38} and Au_{55} clusters. Parts 1.1 and 1.2 show the adsorption sites on Au_{55} and Au_{38} clusters, respectively. Part 1.3 denotes the common TS structure of O_2 dissociation. Parts 2.1 and 2.2 present the adsorption structures of styrene on Au_{55} and Au_{38} clusters, respectively. T, B, and H denote the vertex (or step), bridge, and hollow sites on Au clusters.

of O_2 dissociation at the B_3 site on Au_{38} clusters is also ruled out due to its smaller E_{ad}.

For the adsorption of styrene, different sites on Au_{55} and Au_{38} clusters are calculated. The results show that the most stable adsorption site is the vertex (T_1) on both clusters, as shown in Figures 1.2.1 and 1.2.2. On the Au_{55} cluster, $E_{ad} = 1.26$ eV with the phenyl nearly parallel to the Au surface, which is similar to that on Au(111).[25] Namely, both the C=C bond and the phenyl are interacted with Au atoms. For the Au_{38} cluster, styrene is adsorbed only through the C=C bond to a Au atom with $E_{ad} = 1.23$ eV. Meanwhile, the phenyl tilts to the cluster surface with the tilting angle of about 40°. Because the E_{ad} of styrene is generally several times more than that of O_2 on the identical cluster, O_2 should diffuse to near the styrene under the reaction condition. Therefore, we can get initial structures for the selective oxidation of styrene, which is shown in Figure 2. The styrene is adsorbed on the vertex site while O_2 is adsorbed on the adjacent sites. On the Au_{55} cluster, the only stable structure is present in Figure 2.1 with O_2 adsorbed on the top site. For the Au_{38} cluster, there are two stable structures with O_2 adsorbed on bridge (B_3) or atop (T_1) sites, as shown in Figures 2.2 and 2.3, where the corresponding E_{ad} values (coadsorption energy of O_2 and styrene) of $E_{ad,B3} = 1.22$ eV and $E_{ad,T1} = 1.40$ eV are comparable.

For the epoxidation reaction on the Au_{55} cluster, the minimum energy pathway (MEP) concludes three step reactions with the process of $C_6H_5C_2H_3 + O_2 \rightarrow C_6H_5CHCH_2O_2 \rightarrow C_6H_5CHCH_2O + O \rightarrow C_6H_5CHOCH_2 + O$. The derived values of the first step are $E_{a,1} = 0.79$ eV and $E_{r,1} = -0.27$ eV, whereas the energetic values of the second step are $E_{a,2} = 1.31$ eV and $E_{r,2} = -0.18$ eV. The determined intermediate is an OME structure

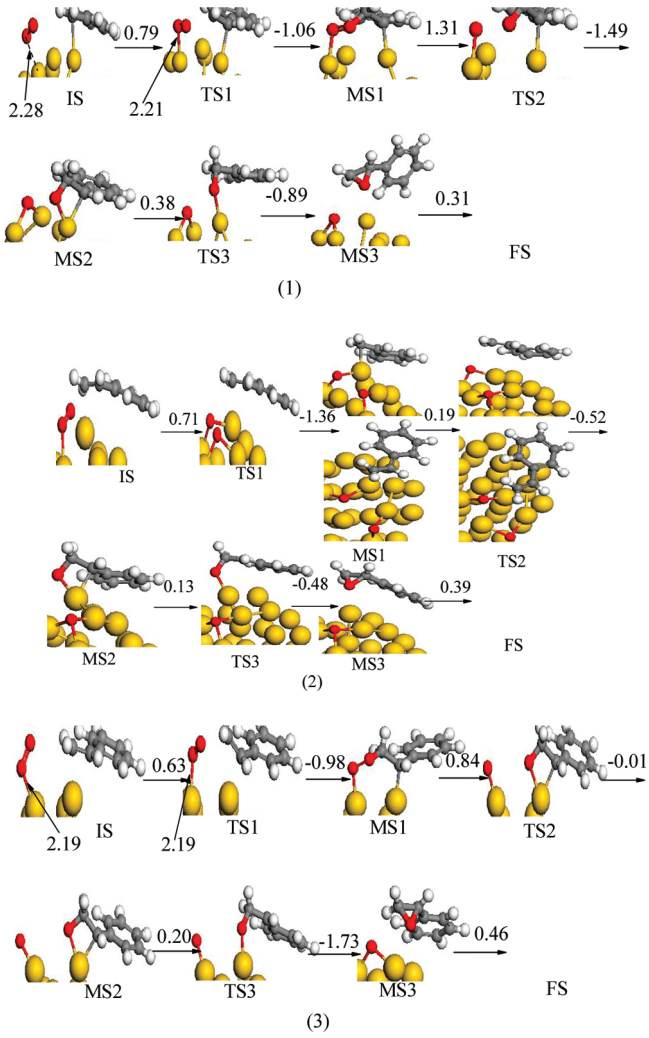

Figure 2. Relative energy diagrams of the styrene epoxidation on Au_{55} and Au_{38} clusters. Diagram 1 shows the reaction process on the Au_{55} cluster, whereas diagrams 2 and 3 show those on the Au_{38} cluster. In diagram 2, both side and top views are displayed for MS1 and TS2.

with its O and C atoms bonding to the common Au atom, which forms C−O−Au−C (MS2), as given in Figure 2.1. This result is consistent with those on Ag_{15} and Ag_{10} clusters.[38] A similar structure has also been found when ethylene is epoxidized on a Ag surface.[39] However, this structure differs from the experimentally and theoretically proposed OMME on Au(111).[24,25] This may be induced by the shape or size difference between a cluster and an extended surface. The probability of this reaction should be little due to their enormous barriers. Thus, the Au_{55} cluster may be inactive or have low activity to the styrene epoxidation.

For the Au_{38} cluster, two different reaction mechanisms are considered: One is that O_2 dissociates before the epoxidation reaction, and another is that O_2 reacts with adsorbed styrene directly. The former mechanism is presented in Figure 2.2. MEP is based on the bridge (B_3) adsorbed O_2 and atop (T_1) adsorbed styrene where $E_a = 0.71$ eV and $E_r = -0.65$ eV for O_2 dissociation. Considering the comparable E_{ad} values between B_3 and T_1 sites, this dissociation reaction should be feasible. Namely, the presence of a preadsorbed styrene on the neighboring Au atom enhances the adsorption possibility of O_2 on the B_3 site as well as its further dissociation. After that, the O atom reacts with styrene through $C_6H_5C_2H_3 + O \rightarrow C_6H_5CHCH_2O$, where $E_{a,1} = 0.19$ eV and $E_{r,1} = -0.33$ eV. Available values are $E_a = 0.42$ eV and $E_r = -0.6$ eV on Au(111),[25] which imply that the Au_{38} cluster is more efficient for epoxidation. The calculated intermediate is also an OME structure, being similar to that on the Au_{55} cluster shown in Figure 2.1. The OME may easily react to $C_6H_5CHOCH_2$ with $E_{a,3} = 0.13$ eV, and the formed $C_6H_5CHOCH_2$ is adsorbed through O to T_1 site. It is observed that the O_2 dissociation is a rate-limiting step (E_a = 0.71 eV). This mechanism agrees with the viewpoint in ref 7 and suggests that Au clusters can dissociate O_2 to yield O adatoms that are necessary for triggering subsequent reactions.

If styrene is epoxidated by O_2 directly on the Au_{38} cluster, the reaction process is similar to that on the Au_{55} cluster. The energetic values are $E_{a,1} = 0.63$ eV, $E_{r,1} = -0.35$ eV, $E_{a,2} = 0.84$ eV, $E_{r,2} = 0.83$ eV, $E_{a,3} = 0.20$ eV, and $E_{r,3} = -1.53$ eV. Obviously, the corresponding E_a values are smaller than those on the Au_{55} cluster, as shown in Figures 2.1 and 2.2. Thus, the Au_{38} cluster is more efficient than the Au_{55} cluster for styrene epoxidation.

The absence of an O_2 dissociation mechanism on the Au_{55} cluster is mainly due to the adsorption property of O_2, which is essentially determined by the structure of the Au cluster. As shown in Figure 1.2, after styrene is adsorbed at the vertex (T_1), both step (T_2) and vertex sites (T_1) are kept beside styrene on the Au_{38} cluster (Figure 1.2.2), while only the step site (T_2) is kept back on the Au_{55} cluster (Figure 1.2.1). Thus, there is only one adsorbed structure for O_2 on the Au_{55} cluster. Moreover, the coordination number (CN) of the step site is 8 on the Au_{38} cluster, whereas that is 9 on the Au_{55} cluster. Hence, there is stronger adsorption of O_2 on the step site of the Au_{38} cluster. Meanwhile, although CN_v (CN at the vertex) of both Au_{38} and Au_{55} clusters are 6, the cohesive energy of the former is lower than that of the latter, as determined in Ag clusters.[40] Namely, the vertex on the Au_{38} cluster is more propitious to adsorb O_2 after styrene is adsorbed. As a result, O_2 could be adsorbed at both T_1 and B_3 sites on the Au_{38} cluster, whereas O_2 would just be adsorbed upright at the T_1 site on the Au_{55} cluster.

To investigate the catalytic mechanism of Au clusters, the changes of electronic structures during the epoxidation process are calculated. For the O_2 dissociation at the B_3 site on the Au_{38} cluster (Figure 2.2), the process is nearly the same as that without styrene (Figure 1.1.3). We define that the O atoms in O_2 near styrene is O2, while another is O1. Correspondingly, the Au atom bonding with O1 is taken as Au1, while that bonding with O2 is named as Au2. In TS1, the O−O bond is stretched while a new Au−O bond (O2−Au2) is formed, where no surface Au atoms are shared between the two O atoms. O and Au hybridize mainly via O 2p orbitals with Au 5d and with additional hybridization of Au 6s during the process in Figure 3. From IS to TS1 to MS1, the hybridization between O 2p and Au 5d is gradually strengthened, while the length of the O2−Au2 bond (L_{O2-Au2}) decreases from 2.36 to 2.24 to 2.19 Å. Meanwhile, O 2s is amalgamated from two separation levels into a single one, which corresponds to the change from the molecular orbital to the atomic orbital. Note that Au 6s has different effects on O1 and O2, which overlaps with O1 2p around −5.71 eV in TS1 (Figure 3.1). In MS1, an O atom is adsorbed through two O−Au bonds at the H_1 site, which further reacts with styrene to form the OME. In this step, the adsorption site of the O atom is changed to the B_2 site in TS2, as shown in Figure 2.2 while the adsorption of styrene is weakened (L_{C-Au2} is changed from 2.22 Å in MS1 to 3.30 Å in TS2). The O−C bond is then built in MS2 (OME), where Au 5d hybridizes with O 2p and C 2p around −6.12 eV, as shown in Figure 4. From OME to TS3, a peak of Au 5d overlaps with O 2p at −1.02 eV

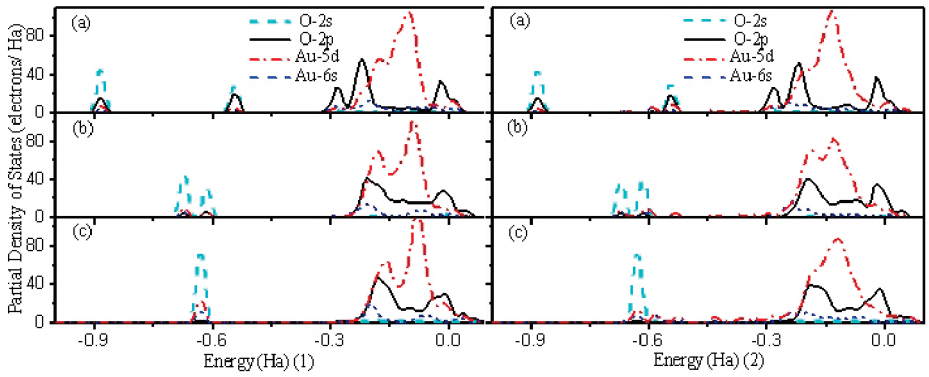

Figure 3. Partial density of states (PDOS) of O_2 dissociation on the Au_{38} cluster before reaction with styrene shown in Figure 2.2. Part 1 (part 2) shows the PDOS of O1 (O2) from panels a to b to c, where a, b, and c denote IS, TS1, and MS1.

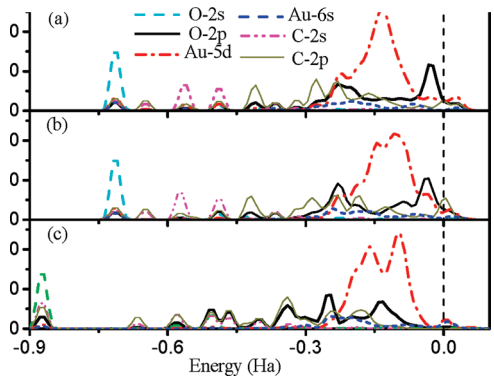

Figure 4. PDOS of O, C, and Au atoms for O reacting with styrene shown in Figure 2.2. a−c denote MS2, TS3, and MS3.

to form an antibonding state, which implies the enhancement of the covalent component of the Au−O bond. On the other hand, the overlap between Au 5d and C 2p is weakened. As a result, L_{Au2-O2} is reduced from 2.14 to 2.09 Å, while L_{Au2-C} increases from 2.27 to 3.08 Å (Figure 2.2). After that, O 2p and O 2s are hybridized with C 2p and C 2s to form MS3, which interacts weakly with Au atoms. Thus, the effect of Au 6s is negligible during the reaction.

For direct reaction of O_2 with styrene, the electronic structures of the reaction process for Au_{38} and Au_{55} clusters are shown in Figure 5. Obviously, the initial half-occupied antibonding orbital $2\pi^*-2p$ of O_2 downshifts from IS to MS1 due to the interaction between Au 5d and $2\pi^*-2p$ of O1−O2. Moreover, the 1π and 5σ states of O1−O2 are notably broadened as the O1−O2 bond weakening from IS to MS1, because the 1π and 5σ states of O1−O2 interact with Au 5d and styrene. As expected, the antibonding $4\sigma^*$ (oxygen lone-pair) state is not involved in the reaction because its position is far below the Fermi level (E_F). As shown in Figure 5b, Au 5d of the Au_{38} cluster has a small peak around E_F compared with that of the Au_{55} cluster, which indicates a stronger hybridization between $2\pi^*2p$ of O1−O2 and Au 5d of the Au_{38} cluster. This can also be proved by $L_{Au(1)-O1}$ of IS and TS1, where $L_{Au(1)-O1}$ values on the Au_{38} cluster (Figure 2.3) are shorter than those on the Au_{55} cluster (Figure 2.1). It was suggested that the high activity of the Au(5,3) nanotube is partially due to the interaction between $2\pi^*2p$ of O1−O2 and Au 5d,[41] which is also the truth for Au clusters. For styrene, the initial empty antibonding orbital π^* is pulled below E_F from IS to MS1 due to the electronic resonance between the antibonding π^* state of styrene and the Au 5d state (Figure 6). Moreover, the peak of Au 5d overlaps with a sharp peak of styrene molecular level at −2.72 eV on the Au_{55} cluster compared with the Au_{38} cluster, which means the stronger interaction between styrene and Au_{55} cluster. As suggested in ref 7, the active clusters should adsorb styrene sufficiently weak that the molecular electronic structure of styrene is not strongly perturbed, which is propitious for epoxidation. Thus, the Au_{38} cluster presents higher catalytic activity for the styrene epoxidation.

For the next step, the O1−O2 bond in $C_6H_5CHCH_2O_2$ is dissociated and meanwhile the O2−Au2 bond is formed. It can be seen that O 2p also mainly hybridizes with Au 5d. From MS1 to TS2, a new peak of O 2p is present around E_F due to the dissociation of the O1−O2 bond, as indicated by the increase of L_{O1-O2}. In TS2, L_{O2-Au} in Au_{55} is 2.70 Å (Figure 2.1) and L_{O2-Au} in Au_{38} is 2.11 Å (Figure 2.3), where the O2−Au bond is formed on the latter. Accordingly, in TS2 (Au_{38}), O 2p overlaps with Au 5d around −1.09 and −6.12 eV while O−S

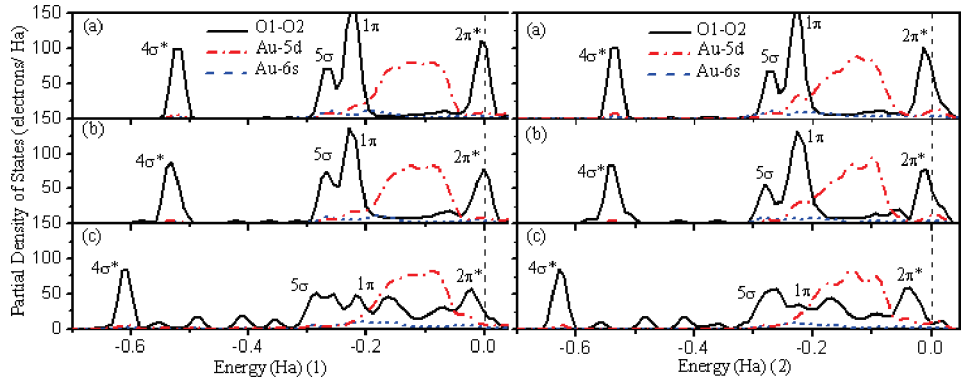

Figure 5. PDOS of O_2 and Au atoms for O2 directly reacting with styrene on Au_{55} (part 1) and Au_{38} (part 2) clusters shown in Figure 2.1. a−c have the same meaning as those in Figure 3.

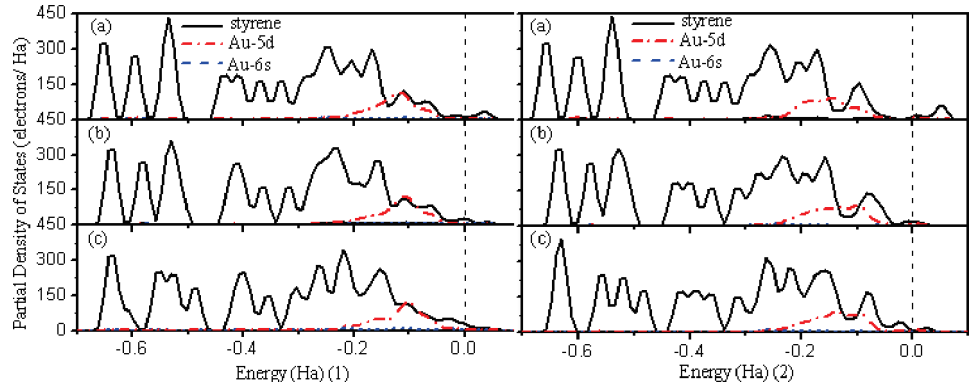

Figure 6. PDOS of styrene and Au atoms for O2 directly reacting with styrene on Au_{55} (part 1) and Au_{38} (part 2) clusters shown in Figure 2.1. a−c have the same meaning as those in Figure 3.

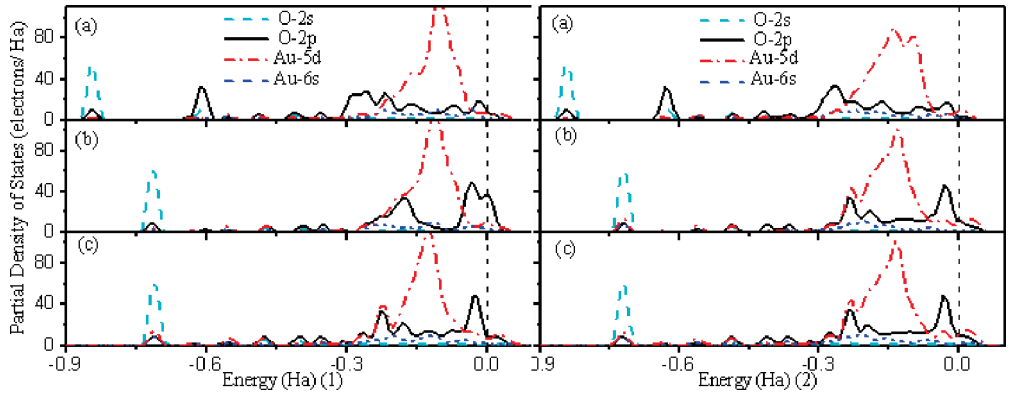

Figure 7. PDOS of O and Au atoms for O1−O2 bond dissociation in $C_6H_5CHCH_2O_2$ on Au_{55} (part 1) and Au_{38} (part 2) clusters shown in Figure 2.1. a−c denote MS1, TS2, and MS2.

TABLE 2: Net Charge of Au and O Atoms at the Reaction Site on Au_{55} and Au_{38} Clusters

	IS		TS1		MS1		TS2		MS2	
	38	55	38	55	38	55	38	55	38	55
Au1	0.129	0.113	0.136	0.135	0.163	0.167	0.283	0.082	0.270	0.199
O1	−0.164	−0.146	−0.204	−0.192	−0.343	−0.347	−0.500	−0.549	−0.502	−0.576
Au2	−0.022	−0.039	0.027	−0.017	−0.026	−0.038	0.124	0.027	0.124	0.122
O2	−0.181	−0.150	−0.178	−0.143	−0.212	−0.187	−0.479	−0.377	−0.288	−0.503

interacts with Au 5d at −19.39 eV, as shown in Figure 7.2. Moreover, in TS2, there is a part of the O 2p peak above E_F on the Au_{55} cluster while a peak of Au 5d is above E_F on Au_{38} cluster. These imply that more net charge transfers from Au 5d to O 2p on the Au_{38} cluster, which is consistent with Mulliken population analysis, as shown in Table 2. In summary, Au 5d, rather than Au 6s, dominates the whole catalytic process through interacting with O_2 and styrene. Moreover, Au1 and Au2 on the Au_{38} cluster surface are more electropositive than those on the Au_{55} cluster surface, as shown in Table 2. Namely, the slightly oxidized gold ($Au^{+\delta}$) is more active, which is in accordance with previous findings.[22,23]

4. Conclusions

In conclusion, the styrene epoxidation on Au_{38} and Au_{55} clusters as well as the corresponding structural and electronic properties is studied by DFT, which find relative energy diagrams of the styrene epoxidation, including active barriers, reactive energies, intermediates, and transition states. The surface oxametallacycle intermediate is OME. The results suggest that the Au_{38} cluster is more likely the size threshold for catalysis with two parallel pathways: O_2 dissociates before epoxidation, and O_2 reacts with styrene directly. The high catalytic activity of the Au_{38} cluster can be understood as follows: For the former, there are different adsorption structures of O_2 and styrene on the Au_{38} cluster due to its geometry. For the latter, the electronic resonance between electronic states of adsorbed intermediate species and Au atoms (mainly 5d states) at the reaction site with a partial charge transfer leads to the results. Moreover, Au atoms correlated with reaction on the Au_{38} cluster are more electropositive than those on the Au_{55} cluster, which is propitious to epoxidation catalysis.

Acknowledgment. We acknowledge support by the National Key Basic Research and Development Program (Grant No. 2010CB631001).

References and Notes

(1) Haruta, M.; Kobayashi, T.; Sano, H.; Yamada, N. *Chem. Lett.* **1987**, *16*, 405.
(2) Haruta, M.; Yamada, N.; Kobayashi, T.; Iijima, S. *J. Catal.* **1989**, *115*, 301.
(3) Sinha, A. K.; Seelan, S.; Tsubota, S.; Haruta, M. *Angew. Chem., Int. Ed.* **2004**, *43*, 1546.
(4) Nijhuis, T. A. R.; Visser, T.; Weckhuysen, B. M. *Angew. Chem., Int. Ed.* **2005**, *44*, 1115.
(5) Abad, A.; Concepción, P.; Corma, A.; Garcia, H. *Angew. Chem., Int. Ed.* **2005**, *44*, 4066.

(6) Chang, F. W.; Yu, H. Y.; Roselin, L. S.; Yang, H. C.; Ou, T. C. *Appl. Catal., A* **2006**, *302*, 157.
(7) Turner, M.; Golovko1, V. B.; Vaughan1, O. P. H.; Abdulkin1, P.; Berenguer-Murcia, A.; Tikhov, M. S.; Johnson1, B. F. G.; Lambert, R. M. *Nature* **2008**, *454*, 981.
(8) Bailie, J. E.; Abdullah, H. A.; Anderson, J. A.; Rochester, C. H.; Richardson, N. V.; Hodge, N.; Zhang, J. G.; Burrows, A.; Kiely, C. J.; Hutchings, G. J. *Phys. Chem. Chem. Phys.* **2001**, *3*, 4113.
(9) Haruta, M. *Catal. Today* **1997**, *36*, 153.
(10) Valden, M.; Lai, X.; Goodman, D. W. *Science* **1998**, *281*, 1647.
(11) Hayashi, T.; Tanaka, K.; Haruta, M. *J. Catal.* **1998**, *178*, 566.
(12) Haruta, M. Catalysis: Gold rush. *Nature* **2005**, *437*, 1098.
(13) Hughes, M. D.; Xu, Y.-J.; Jenkins, P.; McMorn, P.; Landon, P.; Enache, D. I.; Carley, A. F.; Attard, G. A.; Hutchings, G. J.; King, F.; Stitt, E. H.; Johnston, P.; Griffin, K.; Kiely, C. J. *Nature* **2005**, *437*, 1132.
(14) Meier, D. C.; Goodman, D. W. *J. Am. Chem. Soc.* **2004**, *126*, 1892.
(15) Chen, M. S.; Goodman, D. W. *Science* **2004**, *306*, 252.
(16) Chen, M.; Cai, Y.; Yan, Z.; Goodman, D. W. *J. Am. Chem. Soc.* **2006**, *128*, 6341.
(17) Liu, Z.-P.; Jenkins, S. J.; King, D. A. *Phys. Rev. Lett.* **2005**, *94*, 196102.
(18) Liu, Z.-P.; Hu, P.; Alavi, A. *J. Am. Chem. Soc.* **2002**, *124*, 14770.
(19) Bunluesin, T.; Gorte, R. J.; Graham, G. W. *Appl. Catal., B* **1998**, *15*, 107.
(20) Zalc, J. M.; Sokolovskii, V.; Loffler, D. G. *J. Catal. B* **2002**, *206*, 169.
(21) Yoon, B.; Häkkinen, H.; Landman, U.; Wörz, A. S.; Antonietti, J.-M.; Abbet, S.; Judai, K.; Heiz, U. *Science* **2005**, *307*, 403.
(22) Fu, Q.; Saltsburg, H.; Flytzani-Stephanopoulos, M. *Science* **2003**, *301*, 935.
(23) Guzman, J.; Gates, B. C. *Angew. Chem., Int. Ed.* **2003**, *42*, 690.
(24) Deng, X.; Friend, C. M. *J. Am. Chem. Soc.* **2005**, *127*, 17178.
(25) Xue, L.-Q.; Pang, X.-Y.; Wang, G.-C. *J. Comput. Chem.* **2009**, *30*, 438.
(26) Pinnaduwage, D. S.; Zhou, L.; Gao, W. W.; Friend, C. M. *J. Am. Chem. Soc.* **2007**, *129*, 1872.
(27) Delley, B. *J. Chem. Phys.* **1990**, *92*, 508.
(28) Delley, B. *J. Chem. Phys.* **2000**, *113*, 7756.
(29) Hammer, B.; Hansen, L. B.; Nørskov, J. K. *Phys. Rev. B* **1999**, *59*, 7413.
(30) Delley, B. *Phys. Rev. B* **2002**, *66*, 155125.
(31) Benedek, N. A.; Snook, I. K.; Latham, K.; Yarovsky, I. *J. Chem. Phys.* **2005**, *122*, 144102.
(32) Inada, Y.; Orita, H. *J. Comput. Chem.* **2008**, *29*, 225.
(33) Henkelman, G.; Uberuaga, B.; Jonsson, H. *J. Chem. Phys.* **2000**, *113*, 9901.
(34) Chang, C. M.; Cheng, C.; Wei, C. M. *J. Chem. Phys.* **2008**, *128*, 124710.
(35) Barton, D. G.; Podkolzin, S. G. *J. Phys. Chem. B* **2005**, *109*, 2262.
(36) Deng, X. Y.; Min, B. K.; Guloy, A.; Friend, C. M. *J. Am. Chem. Soc.* **2005**, *127*, 9267.
(37) Lopez, N.; Nørskov, J. K. *J. Am. Chem. Soc.* **2002**, *124*, 11262.
(38) Enever, M.; Linic, S.; Uffalussy, K.; Vohs, J. M.; Barteau, M. A. *J. Phys. Chem. B* **2005**, *109*, 2227.
(39) Mavrikakis, M.; Doren, D. J.; Barteau, M. A. *J. Phys. Chem. B* **1998**, *102*, 394.
(40) Liu, D.; Zhu, Y. F.; Jiang, Q. *J. Phys. Chem. C* **2009**, *113*, 10907.
(41) An, W.; Pei, Y.; Zeng, X. C. *Nano Lett.* **2008**, *8*, 1195.

JP909345J